

Branched Multi-Task Networks: Deciding What Layers To Share

Simon Vandenhende¹ Bert De Brabandere¹ Luc Van Gool^{1,2}

¹KU Leuven - ESAT-PSI ²ETHZ - CVL

{simon.vandenhende, bert.debrabandere, luc.vangool}@esat.kuleuven.be

Abstract

In the context of deep learning, neural networks with multiple branches have been used that each solve different tasks. Such ramified networks typically start with a number of shared layers, after which different tasks branch out into their own sequence of layers. As the number of possible network configurations is combinatorially large, prior work has often relied on ad hoc methods to determine the level of layer sharing.

This work proposes a novel method to assess the relatedness of tasks in a principled way. We base the relatedness of a task pair on the usefulness of a set of features of one task for the other, and vice versa. The resulting task affinities are used for the automated construction of a branched multi-task network in which deeper layers gradually grow more task-specific. Our multi-task network outperforms the state-of-the-art on CelebA. Additionally, the layer sharing schemes devised by our method outperform common multi-task learning models which were constructed ad hoc. We include additional experiments on Cityscapes and SUN RGB-D to illustrate the wide applicability of our approach. Code and trained models for this paper are made available.¹

1. Introduction

Deep neural networks are usually trained to tackle specific, isolated tasks. Humans, in contrast, are remarkably good at solving a wide range of diverse tasks concurrently. Biological data processing appears to follow a multi-tasking strategy. Instead of separating tasks and solving them in isolation, different processes seem to share the same early processing layers in the brain (e.g. V1 in macaques [13]). Similarly, deep learning researchers have begun to develop deep neural networks with multiple branches, that each solve different tasks.

Multi-task networks [5] seek to improve generalization and processing efficiency through the joint learning of related tasks. Compared to the typical learning of separate

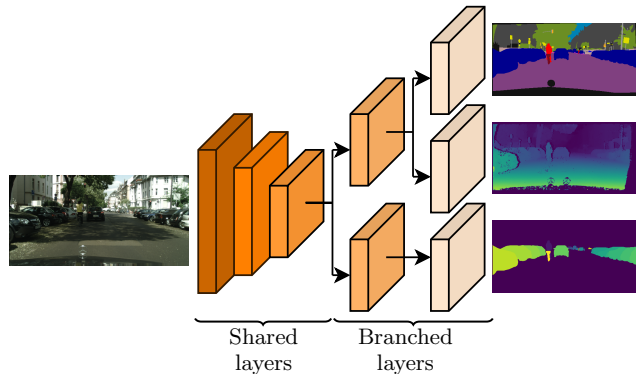


Figure 1: **A branched multi-task network:** The bottom layers are shared by all tasks, while later layers split off as they show more task-specific behavior.

deep neural networks for each of the individual tasks, multi-task networks come with several advantages. First, due to the sharing of layers, the resulting memory footprint typically is substantially lower [12, 24, 25, 33, 38]. Secondly, because features in the shared layers do not need to be calculated repeatedly for the different tasks the overall calculation speed is often higher [38, 41]. Finally, a multi-task network may outperform networks trained for the tasks individually [5, 24, 49].

In the context of deep neural networks, we can discriminate between two main paradigms for multi-task learning. In the first setting - named hard parameter sharing - the input is first encoded through a shared network of layers after which tasks branch out into their own sequence of task-specific layers [12, 24, 25, 38, 49, 60]. Alternatively, a set of task-specific networks can be used in combination with a feature sharing mechanism. The latter approach is termed soft parameter sharing [33, 40, 48].

This paper focuses on the hard parameter sharing model. A significant challenge is to decide on the layers that need to be shared amongst tasks. Since the number of possible configurations grows quickly with the number of tasks, a trial-and-error procedure becomes unwieldy. Most previous

¹<https://github.com/SimonVandenhende/>

works opt for the simple strategy of sharing the initial layers in the network, after which all tasks branch out simultaneously. The point at which the branching occurs is usually determined ad hoc. This situation hurts performance, as a suboptimal grouping of tasks can lead to the sharing of information between unrelated tasks. This is referred to as negative transfer.

This work aims to find principled ways to decide on the degree of layer sharing between tasks, eliminating the need for manual exploration. To this end, we base the sharing of layers on measurable levels of *task affinity* or *task relatedness*. We define two tasks as strongly related, if their single task models rely on a similar set of features. We quantify this property by measuring the performance when solving a task with variable sets of layers of a model from a different task. In particular, suppose we have two tasks a, b and their corresponding single task models M_a, M_b . We hypothesize that when task a can be solved more easily by using features extracted by a set of layers from M_b , and vice versa, task a and b should be scored more related. We assess the task affinity at varying depths in the network by repeating the experiment with different sets of layers from M_a and M_b . This gives us a three-dimensional tensor of normalized task affinity scores. The tensor values are used to cluster related tasks together by trading off network complexity against task affinity. In short, our contributions are:

- Given a dataset and a number of tasks, we propose a novel method to assess the task affinity. In particular, an affinity measure is introduced to judge the relatedness of tasks at arbitrary locations in a neural network.
- The task affinity scores are used to construct a branched multi-task network in a fully automated manner. Our task clustering algorithm separates dissimilar tasks by assigning them to different branches, thereby reducing the negative transfer between tasks. Additionally, our method allows to trade network complexity against task similarity.
- We provide extensive empirical evaluation of our method. The learned task groupings outperform the state-of-the-art on CelebA. Furthermore, we apply our method to Cityscapes and SUN RGB-D to show its wide applicability. In particular, we find that the layer sharing schemes devised by our method outperform common multi-task learning models which were constructed ad hoc.

2. Related work

Multi-task learning Multi-task learning (MTL) [5, 47] has been studied for a long time. Models for MTL can typically be classified as utilizing hard or soft parameter sharing. In hard parameter sharing, the parameter set is divided

into a shared and task-specific set of parameters. In soft parameter sharing, each task is assigned its own set of parameters, but part of the parameter set is constrained through a Bayesian prior [56].

Early work on multi-task learning often relied on a sparsity constraint [3, 22, 34, 37, 57] to select a small subset of features that could be shared amongst all tasks. This can lead to a negative transfer when not all tasks are related to each other. A general solution to the problem is to cluster tasks based on prior knowledge about their similarity [1, 2, 11, 26, 61].

In the context of deep learning, we find that MTL models are often based on a shared off-the-shelf encoder followed by task-specific decoder networks [6, 24, 41, 49]. Multilinear relationship networks [36] extend this general framework by placing tensor normal priors on the parameter set of the fully connected layers. Guo et al. [12] proposed the construction of a hierarchical network, which predicts increasingly difficult tasks at deeper layers. Our branched multi-task networks use a tree-based hard parameter sharing model. Furthermore, the degree to which layers are shared is determined in a principled way.

Cross-stitch [40] networks softly share their features amongst tasks, by using a linear combination of the activations found in multiple single task network. Both cross-stitch and cross-connected networks are limited in terms of scalability, as the size of the network tends to grow linearly with the number of tasks. Sluice networks [48] extend cross-stitch networks and allow to learn the selective sharing of layers, subspaces and skip connections. Multi-task attention networks [33] use an attention mechanism to share a general feature pool amongst task-specific networks.

The joint learning of multiple tasks requires to combine the loss functions associated with the individual tasks. Early work [24] used the homoscedastic uncertainty of each task to weigh the losses. Gradient normalization [6] balances the learning of tasks by dynamically adapting the gradient magnitudes in the network. Sener et al. [49] cast multi-task learning as a multi-objective optimization problem, with the overall objective of finding a Pareto optimal solution. Dynamic task prioritization [12] prioritizes the learning of difficult tasks. Zhao et al. [60] observed that two competing tasks can cause the destructive interference of the gradient. A modulation module is proposed to alleviate the gradient interference problem. The experiments in this work are based on a simple uniform loss weighing scheme. We show that even with such a naive loss weighing, a branched multi-task network can improve performance when compared against a set of task isolated models.

Multi-attribute learning We consider multi-attribute learning [4, 15] a special case of multi-task learning, where each attribute is treated as a separate task, as in [38, 46, 49].

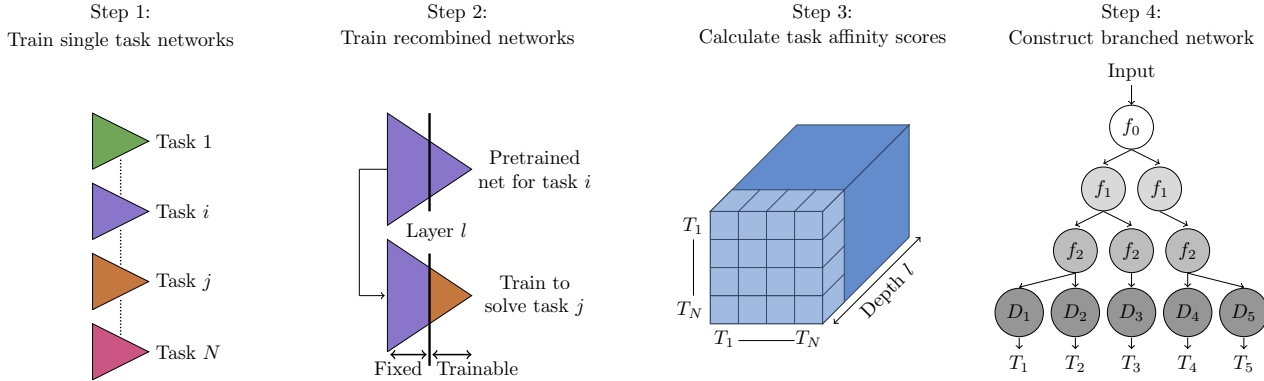


Figure 2: **We construct a branched multi-task network based on measurable task affinity scores.** The method consists of four steps. (1) Train single task models for the tasks in \mathcal{T} . The single task models are comprised of an identical encoder and a small task-specific decoder. (2) Split the encoder into a fixed and trainable part. The trainable part is retrained to solve its original task, this time using the features that are extracted by the fixed part of a different single task model. We repeat this process for all pairs of tasks, effectively solving tasks with features originally extracted for the other tasks in \mathcal{T} . Afterwards, we make the split at various other locations. (3) Calculate the task affinity scores based on the usefulness of features from one task to solve the others. To this end, we consider the performance that is obtained with the recombined networks from the previous step. (4) Construct a branched multi-task network based on the measured levels of task affinity.

A greedy neural network search strategy tailored to multi-attribute learning was proposed by [20]. Fully-adaptive feature sharing [38] starts from a thin network in which tasks initially share all layers but the final one. The model is grown dynamically during training, in a greedy layer-by-layer fashion, taking into account task affinity. Similarly, our method clusters tasks based on affinity scores. We calculate the scores in a novel way before training the MTL model. Additionally, we take into account the affinity at multiple successive layers during the clustering process.

Neural architecture search Recent work [29] implemented an evolutionary architecture search for multi-task networks. Neural architecture search [10] (NAS) aims to automate the construction of the network architecture. Different algorithms can be characterized based on their search space, search strategy or performance estimation strategy. Most work on NAS is limited to task-specific models [31, 32, 43, 44, 62]. In contrast to NAS, we do not build the architecture from scratch, but start from a predefined network for which we determine a layer sharing scheme.

Transfer learning Transfer learning [42] leverages the knowledge obtained in one task domain, to solve a new task on a similar domain. Taskonomy [58] provides a taxonomy for task transfer learning which is based on measurable task relationships. We use the performance metric from their work to compare the usefulness of different feature sets to solve a task.

Model compression The parameter-sharing schemes in MTL can also be seen as a form of model compression, which aims to lower memory and computation requirements. Other model compression methods involve pruning and sharing [14, 16, 28, 39], low-rank-factorization [21, 53], knowledge distillation [18, 45] and transferred convolutional features [7, 9, 27]. Most of these methods function task independently and can complement our method to further reduce the model size.

3. Method

Suppose we aim to jointly solve N different tasks $\mathcal{T} = \{t_1, \dots, t_N\}$ with a multi-task network. The architecture consists of a sequence of shared layers or blocks f_l , followed by one or more task-specific layers. We assume an appropriate structure for sharing the layers to take the shape of a tree. In particular, the bottom layers are shared by all tasks, while later layers split off as they show more task-specific behavior. The proposed method aims to decide on an effective task grouping for the sharable layers f_l , i.e. grouping similar tasks together in the same branch of the tree.

When two tasks are strongly related, we expect their single task models to rely on a similar feature set. Based on this viewpoint, the proposed method derives a task affinity score at various locations in the model. The resulting task affinity scores are used to construct a branched multi-task network. The method consists of four steps illustrated and summarized in figure 2.

3.1. Step 1: Train single task networks

As a first step, we train a task-specific model for each task $t_i \in \mathcal{T}$. The single task models use an identical encoder E - made of the sharable layers f_l - followed by a task dependent decoder D_{t_i} . The decoder contains task-specific operations and is assumed to be much smaller than the encoder. As an example, consider jointly solving a classification and dense prediction task. An additional decoding step is needed for the dense prediction task, in comparison to the classification task. Such up or down scaling operations are part of the task-specific decoder D_{t_i} . The different single task networks are trained under the same conditions.

3.2. Step 2: Train recombined networks.

Consider a task t_i in \mathcal{T} . We reuse the corresponding single task model from the previous step, but substitute the bottom l layers with their pretrained equivalent found in one of the other single task networks. The resulting model is retrained to solve its original task t_i , while keeping the weights of the substituted layers fixed. This forces the model to solve task t_i based on features that were initially extracted to solve a different task. The performance difference compared to the single task model will serve as a measure for task affinity in the third step. We recombine the single-task networks from before for all possible pairs of tasks and fine tune the resulting networks for one of both tasks, while keeping the features borrowed from the other task fixed.

More concretely, we sample two tasks t_i and t_j from \mathcal{T} . We define the fixed part of the model as the bottom l layers of the model trained to solve task t_j . The trainable part of the model comprises the remaining layers of the sharable encoder and the task-specific decoder D_{t_i} for task t_i . The trainable part of the model learns to solve task t_i using features from task t_j , which are extracted by the fixed part of the model. We repeat the described procedure N^2 times to cover each pair of tasks $t_i, t_j \in \mathcal{T}$. The locations l at which we split the sharable encoder E are dependent on the architecture. More details on where to split the encoder are given in the experiments section. We provide details on the computational budget that is needed in section 4.5. The training hyperparameters remain the same as in step one.

3.3. Step 3: Calculate task affinity scores

In the third step, we calculate the task affinity scores based on the performance of the recombined networks trained in the previous step. When two tasks are strongly related, we expect their single task models to rely on a similar set of features. Concretely, we hypothesize that the pair of tasks t_i, t_j should be scored more related when features of task t_i are helpful for solving task t_j , and vice versa. To assess the task affinity requires to score the transfer characteristic when using features from different tasks. We adapt

the method from [58] to obtain a performance score for each separate encoder. Given the importance of the performance scores for our further analysis, we briefly describe the method in the next paragraph.

For each task t_l , we construct a pairwise tournament matrix W_{t_l} between all tasks in \mathcal{T} . The elements w_{ij} represent the fraction of samples for which the encoder from task t_i results in a lower loss, compared to the encoder from task t_j for solving task t_l . We retrieve the final performance vector for task t_l by normalizing the principal eigenvector of W_{t_l} . The relative performance score of the encoder from task t_i corresponds to the i^{th} component of the normalized eigenvector. The performance matrix P is found by stacking the performance vectors for all tasks $t_l \in \mathcal{T}$.

We defined task relatedness as the degree to which two tasks rely on a similar set of features. Concretely, this means that for a pair of related tasks, we expect the encoder of one task to be helpful in solving the other, and vice versa. This leads us to define the symmetric task affinity matrix as $A = \frac{1}{2} (P + P^T)$. We repeat this procedure at various depths in the sharable part of the model. This gives us an affinity score at an arbitrary location in the network, quantifying how similar a pair of tasks is at a certain depth. The task affinity scores are represented by a tensor of size $N \times N \times L$, with N the number of tasks and L the number of locations at which we split the sharable encoder.

3.4. Step 4: Construct a branched multi-task network

Representation As a final step, we use the task affinity scores to derive how the layers or blocks f_l in the encoder E should be shared amongst the tasks in \mathcal{T} . Since we assume an appropriate layer sharing scheme to take the shape of a tree, we now link the most common hierarchical tree concepts with our approach.

Each layer or block $f_l \in E$ is represented as a node in the tree, i.e. the root node contains the first layer or block f_0 and nodes at depth l contain f_l . The granularity of the building blocks f_l corresponds to the intervals at which we split the sharable part of the model during the second step. When the encoder is split into b_l branches at depth l , this is equivalent to a node at depth l having b_l children. The task-specific decoders D_t can be found in the leaves of the tree. Figure 2 shows an example of a tree using the proposed notation. Each node is responsible for solving a unique set of tasks.

Clustering the affinity tensor into task groupings The task affinity tensor is used to derive a tree. Inspired by [38], we weigh the task affinity scores against network complexity to derive the task grouping. Opposed to their work, the task affinity scores are determined before training the MTL

network. As a result, given a task grouping, we can calculate its cost a priori.

Assume we cluster the tasks at layer l . We can perform spectral clustering for each possible number of groups m with $1 \leq m \leq b_{l+1}$ and b_{l+1} the number of branches at layer $l+1$. The cost of a task grouping g at layer l is defined as

$$C^l(g) = C_{clustering}^l(g) + \alpha \cdot C_{complexity}^l(g). \quad (1)$$

The *clustering cost* $C_{clustering}^l(g)$ at depth l is found by averaging the maximum distance between the elements in the cluster. This encourages the optimization procedure to separate dissimilar tasks. The distance is calculated using the affinity scores that were measured at layer l during the third step. Tuning the *complexity parameter* α allows to trade network complexity against task affinity. The *complexity cost* $C_{complexity}^l$ at depth l is defined similarly to [38],

$$C_{complexity}^l(g) = (b_l - 1) \cdot 2^{p_l} \quad (2)$$

with b_l the number of branches at depth l and p_l the number of pooling layers above layer l . In case we are using a model with dilated convolutions, rather than pooling layers, we base the number p_l on the resolution of the activation maps. Intuitively, the complexity cost increases with the number of branches. We assign a higher cost to creating a new branch when it operates before a down sampling operation.

The cost of a tree is found by summing the costs of its associated task grouping g at all depths l . The final model is obtained when we find the tree with minimal cost. When the number of tasks is large, e.g. on CelebA, an exhaustive search becomes intractable. We propose to construct the model in a top-down manner, starting at the most outer layer or block. At every step, we select the top- n task groupings with minimal cost. This constrains the number of possible groupings at the next layer. When we proceed to the next layer, we choose the top- n groupings from the ones that can still be constructed. At layer l , we calculate the cost of a task grouping by taking the sum for all layers $i \geq l$. Our procedure aims to find a task grouping which is considered better globally, rather than a grouping which is only optimal at a specific depth. This approach is inspired by [47], where mention was made about the approach from [38] being only optimal at the level of isolated layers. We provide more details on choosing the value of n in section 4.5.

4. Experiments

4.1. CelebA

Dataset The CelebA [35] dataset contains over 200k images of celebrities labeled with 40 facial attribute categories. The training, validation and test set contain 160k,

20k and 20k images respectively. We treat the prediction of each facial attribute as a single task, as in [20, 38, 49].

Training procedure We use the thin- ω model from [38] in our experiments on CelebA. The neural network is based on the VGG-16 model [51]. The number of convolutional features is set to the minimum between ω and the width of the corresponding layer in the VGG-16 model. The fully connected layers contain $2 \cdot \omega$ features.

To ensure a fair comparison with earlier work, we set the value of the complexity parameter α and the width of the network ω such that the resulting model contains a comparable amount of parameters as prior work. We measure the task affinity after every layer. The branched multi-task network is trained using stochastic gradient descent with momentum 0.9 and initial learning rate 0.05. We use batches of size 32 and weight decay 0.0001. The model is trained for 120000 iterations and the learning rate divided by 10 every 40000 iterations. The loss function is a sigmoid cross-entropy loss with uniform weighing scheme.

Results Table 1 shows the performance on the test set. The branched multi-task model outperforms earlier work [20, 38] on CelebA. Since our Thin-32 model only differs from the model of [38] on the task clustering, we can conclude that the proposed method devises effective task groupings on CelebA. Interestingly, our Thin-32 model performs on par with the VGG-16 baseline, while using 64 times less parameters. We show the learned task grouping in figure 3.

We compare our approach with cross-stitch networks [40] for a moment. While the latter suffers from scalability issues, our method uses the parameter set more efficiently. This becomes particularly clear on the CelebA dataset. While a cross-stitch network would use 40 times the amount of parameters as the thinned VGG-16 model, our Thin-32 model only uses a factor of 10. Additionally, tuning the parameter α gives our approach more freedom in choosing the number of parameters.

Dynamic growing Earlier work [38] determined the task affinity during the training of the MTL model. This requires to start from a thin model, in which tasks initially share all layers, and dynamically grow the model as training proceeds. Our method calculates the task affinity scores beforehand, which obviates the need to dynamically grow the model. We compared results for both cases when using our task affinity scores and found that the dynamically grown model performs 0.14% better on the test set. Since the layers are initially trained with all the available training signals, dynamically growing the model might give the usual benefits of pre-training.

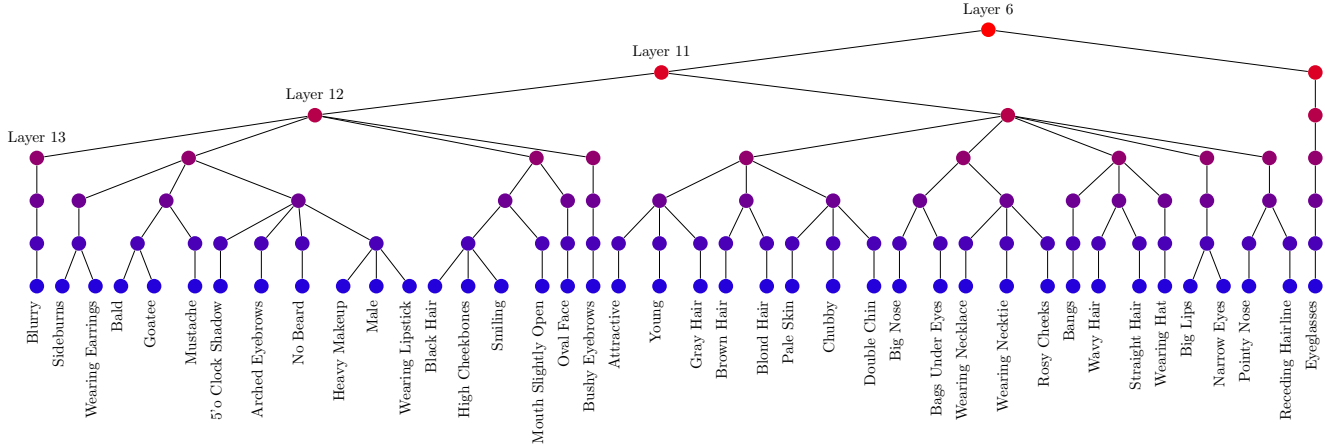


Figure 3: Grouping of person attribute classification tasks on CelebA in a thin VGG-16 architecture.

Method	Acc (%)	Params (10^6)
LNet+ANet [54]	87	-
Walk and Learn [54]	88	-
MOON [46]	90.94	119.73
Independent Group [15]	91.06	-
MCNN [15]	91.26	-
MCNN-AUX [15]	91.29	-
VGG-16 Baseline [38]	91.44	134.41
Branch-32-2.0 [38]	90.79	2.09
GNAS-Shallow-Thin [15]	91.30	1.57
<i>GNAS-Shallow-Wide [15]</i>	<i>91.63</i>	<i>7.73</i>
GNAS-Deep-Thin [15]	90.90	1.47
GNAS-Deep-Wide [15]	91.36	6.41
Ours-Thin-32	91.45	2.20
<i>Ours-Thin-60</i>	<i>91.73</i>	<i>7.73</i>

Table 1: Performance on the CelebA test set. **(bold)** The complexity parameter α is selected to give the Thin-32 model a comparable amount of parameters as the Branch-32-2.0 model. Consequently, our Thin-32 model only disagrees with the Branch-32-2.0 on the task grouping. *(italic)* The Thin-60 model is the result of widening the Thin-32 model until it matches the number of parameters in the GNAS-Shallow-Wide model.

4.2. Cityscapes

Dataset The Cityscapes dataset [8] considers urban scene understanding. The train, validation and test set contain 2975, 500 and 1525 images respectively. We consider the tasks of semantic segmentation, instance segmentation and monocular depth estimation. The dataset has annotations for 19 semantic classes. The depth maps were labeled using SGM [19].

Training procedure We implement the same network architecture, loss function and hyperparameter search as earlier work [49]. We use an MSE loss to estimate the disparity, which is later converted to a depth map using the included camera parameters. The semantic segmentation task is learned with a pixel-wise cross-entropy loss. We reuse the approach from [24] for the instance segmentation task, i.e. we consider the proxy task of regressing each pixel to the center of the instance it belongs to. All images are rescaled to 256 by 512 pixels.

A ResNet-50 [17] with dilated convolutions is used as architecture for the sharable encoder. All tasks use a pyramid pooling module [60] as task-specific decoder. The task affinity is measured after each block in the ResNet-50 encoder. We follow the procedure from [49] and use the Cityscapes validation images as our test set. In particular, we estimate the hyperparameters on a subset of the train images after which we retrain on the entire train set.

Results We set the complexity parameter α to 0.2 when clustering the tasks. Figure 4a shows the learned task grouping. Our method decides to split off tasks after the third residual block. This contrasts with earlier work [24, 49], which shares the complete ResNet-50 encoder. We report the performance on the Cityscapes validation set in table 2. Our branched multi-task network outperforms the single task models, while trained with a simple uniform loss weighing. Furthermore, while the baseline MTL model suffers from a negative transfer, this effect is kept under control in the branched multi-task model. Our method seems to effectively separate dissimilar tasks by assigning them to different branches.

We compare our results with prior work on multi-task learning architectures. The MTAN model [33] only considers the semantic segmentation and depth estimation tasks

Method	S (IoU)	I (px)	D (px)	#P
Single Task [49]	60.68	11.34	2.78	138
Baseline MTL [49]	54.59	10.38	2.95	92
Branched MTL	61.35	9.96	2.66	107

Table 2: Performance on the Cityscapes validation set. The multi-task learning models were trained with a uniform loss weighing scheme. We report the performance for the semantic segmentation (S), instance segmentation (I) and monocular depth estimation task (D). The number of parameters is expressed in millions.

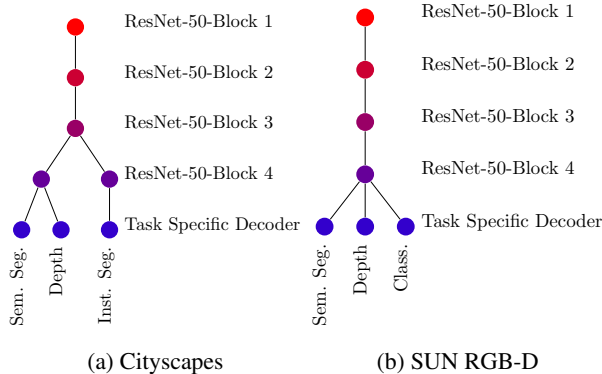


Figure 4: Layer sharing scheme on Cityscapes and SUN RGB-D. On the Cityscapes dataset, we consider the semantic segmentation, instance segmentation and monocular depth estimation tasks. On the SUN RGB-D dataset, we consider the semantic segmentation, scene categorization and monocular depth estimation tasks.

on Cityscapes. This task pair is closely related according to our task affinity measure. The task hierarchy in [12] orders tasks based on their difficulty. This model also outperforms the baseline hard parameter sharing model, while using the parameter set efficiently. In contrast to our method, the model structure needs to be determined through a trial-and-error process.

4.3. SUN RGB-D

Dataset The SUN RGB-D dataset [23, 50, 52, 55] contains 10335 images of indoor scenes. All images have annotations for semantic segmentation, scene categorization and monocular depth estimation. We follow the approach from [52] for the scene categorization task, i.e. we only consider categories with more than 80 samples. The remaining images are categorized under the class *other*, for which we set the class weight equal to zero. All images are rescaled to 480 by 640 pixels. We opt for a simple augmentation strategy and only include random horizontal flipping.

Layer	Features
Conv(k=3,p=1,s=1) + BN + ReLU	512
Conv(k=3,p=1,s=2) + BN + ReLU	128
Conv(k=3,p=0,s=0)	1

Table 3: Task-specific decoder for the scene categorization task on SUN RGB-D.

Training procedure We reuse the ResNet-50 model as our sharable encoder network. The weights are again initialized on ImageNet. The semantic segmentation and monocular depth estimation task use a pyramid pooling module as task-specific decoder. The scene categorization task uses a simple convolutional decoder (see table 3). The task affinity is again calculated after each ResNet block. We use an SGD optimizer with momentum 0.9, initial learning rate 0.001 and a batchsize of 8. The model is trained for 70 epochs and the learning rate divided by 10 every 30 epochs.

Results The complexity parameter α is set to the same value as before. The learned task grouping is shown in figure 4b. The tasks on SUN RGB-D are considered closely related by the task affinity measure. This results in the complete encoder being shared amongst all tasks. Table 4 reports the performance on the test set. The constructed MTL model performs on par with the single task models for semantic segmentation and monocular depth estimation, while outperforming the scene categorization model. The branched multi-task model uses only 63 % of the number of parameters in comparison to the combination of the single task models.

Comparison with tasks on Cityscapes We compare the task affinity at different locations in the network between the tasks on SUN RGB-D and Cityscapes in figure 5. The tasks on SUN RGB-D are scored more strongly related in the deeper layers. We find that the task affinity scores can provide clues about the performance of a multi-task network which shares the entire encoder. In particular, such a task grouping leads to a significant performance decrease on Cityscapes, while being an effective grouping for the tasks on SUN RGB-D.

4.4. Repeatability of task groupings

Are the discovered task groupings repeatable, i.e. does a small change in the training procedure of the recombined networks lead to a completely different grouping of tasks or not? We retrained the recombined networks on Cityscapes under several conditions - using a different optimizer (SGD/Adam) and using half versus the complete training set. The task clustering procedure resulted in the

Method	S (IoU)	D (m)	C (%)	#P
Single Task	41.01	0.344	63.31	125
RefineNet [30]	45.7	-	-	118
Task-Recursive [59]	46.3	0.219	-	-
MTL (ours)	40.65	0.349	66.75	79

Table 4: Results on the SUN RGB-D test set. Our branched multi-task learning model is trained with a uniform loss weighing scheme. We report the performance for the semantic segmentation (S), monocular depth estimation (D) and scene categorization tasks (C). The number of parameters is expressed in millions.

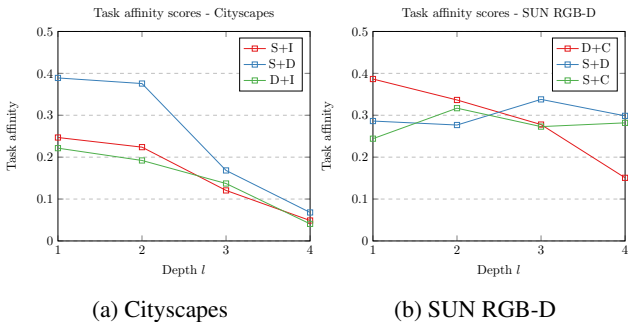


Figure 5: Task affinity on Cityscapes and SUN RGB-D as a function of depth. The tasks on SUN RGB-D are found to be more strongly related by the task affinity metric.

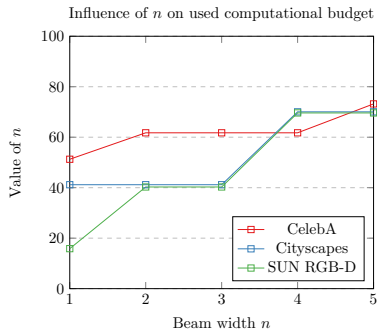


Figure 6: Computational budget required to retrieve the necessary task affinity scores in comparison to retrieving them for all N tasks at L locations.

same tree structure on every run. Furthermore, the relative ordering of task similarities remained the same in 86.2 percent of the cases. This means, when there are two task pairs of which one is more strongly related, our method is likely to yield that conclusion even when trained under different conditions. Furthermore, the task affinity scores can be calculated using a subset of the available training data. This is a simple way to reduce the computational budget.

The repeatability of the task groupings should in fact not come as a surprise. Earlier work [58] assessed the performance of networks where the encoder and decoder were recombined to model task transfer relationships. They came to a similar conclusion, i.e. the performance score of the recombined networks is rather robust.

4.5. Computational budget

The proposed method requires to obtain N^2 encoder-decoder pairs, split at L different locations. Training the recombined models on a server with two Tesla P-100 GPUs takes roughly two days for the tasks on Cityscapes and SUN RGB-D. Notice that we apply early stopping, as the models which were split in the deeper layers converge rather rapidly. Furthermore, as discussed in section 4.4, the computational budget can be further reduced by calculating the task affinity scores using only a subset of the available training data.

In our experiments, the tasks are merged into a single branch beyond a particular layer. This causes the clustering procedure to end. When this occurs in all top- n groupings, calculation of the task affinities at lower layers can be omitted. We plot the reduction in train time as function of the parameter n in figure 6. The computational budget for obtaining the necessary encoder-decoder pairs can be reduced. On Cityscapes and SUN RGB-D, n is set to one. While for CelebA we set n equal to three. Notice that the value of n mainly depends on the scale at which we recombine the networks. If this happens at very fine-grained intervals, relative changes in affinity are smaller and more susceptible to noise. In this case, choosing $n > 1$ can help.

5. Conclusion

We considered the use of branched multi-task networks in which deeper layers gradually grow more task-specific. Additionally, we introduced a principled method to construct such branched multi-task networks. Our construction process groups related tasks together by making a trade-off between task similarity and network complexity. The task affinity scores are based on the premise that similar tasks can be solved with a similar set of features. In contrast to prior work [38], we show that our method can be applied to a wide variety of tasks, ranging from multi-attribute prediction to the combination of scene categorization and dense prediction tasks. Future work should extend our approach to allow more freedom in the construction of individual branches. Furthermore, it would be interesting to see which loss weighing schemes fit best with our approach.

Acknowledgments

This work was financed by Interl Funds KU Leuven (C14/18/065) and is part of the MACCHINA project. We

would like to thank Ali Diba, Davy Neven, Marc Proesmans and José Oramas M. for helpful discussions. We thank Sensifai for providing computational facilities.

References

- [1] J. Abernethy, F. Bach, T. Evgeniou, and J.-P. Vert. A new approach to collaborative filtering: Operator estimation with spectral regularization. *JMLR*, 10(Mar):803–826, 2009. 2
- [2] A. Agarwal, S. Gerber, and H. Daume. Learning multiple tasks using manifold regularization. In *NIPS*, 2010. 2
- [3] A. Argyriou, T. Evgeniou, and M. Pontil. Multi-task feature learning. In *NIPS*, 2007. 2
- [4] J. Cao, Y. Li, and Z. Zhang. Partially shared multi-task convolutional neural network with local constraint for face attribute learning. In *CVPR*, 2018. 2
- [5] R. Caruana. Multitask learning. *Machine learning*, 28(1):41–75, 1997. 1, 2
- [6] Z. Chen, V. Badrinarayanan, C.-Y. Lee, and A. Rabinovich. Gradnorm: Gradient normalization for adaptive loss balancing in deep multitask networks. In *ICML*, 2018. 2
- [7] T. Cohen and M. Welling. Group equivariant convolutional networks. In *ICML*, 2016. 3
- [8] M. Cordts, M. Omran, S. Ramos, T. Rehfeld, M. Enzweiler, R. Benenson, U. Franke, S. Roth, and B. Schiele. The cityscapes dataset for semantic urban scene understanding. In *CVPR*, 2016. 6
- [9] S. Dieleman, J. De Fauw, and K. Kavukcuoglu. Exploiting cyclic symmetry in convolutional neural networks. In *ICML*, 2016. 3
- [10] T. Elsken, J. H. Metzen, and F. Hutter. Neural architecture search: A survey. *arXiv preprint Arxiv:1808.05377*, 2018. 3
- [11] T. Evgeniou and M. Pontil. Regularized multi-task learning. In *ACM SIGKDD*, 2004. 2
- [12] M. Guo, A. Haque, D.-A. Huang, S. Yeung, and L. Fei-Fei. Dynamic task prioritization for multitask learning. In *ECCV*, 2018. 1, 2, 7
- [13] M. Gur and D. M. Snodderly. Direction selectivity in v1 of alert monkeys: evidence for parallel pathways for motion processing. *The Journal of physiology*, 585(2):383–400, 2007. 1
- [14] S. Han, H. Mao, and W. J. Dally. Deep compression: Compressing deep neural networks with pruning, trained quantization and huffman coding. *arXiv preprint arXiv:1510.00149*, 2015. 3
- [15] E. M. Hand and R. Chellappa. Attributes for improved attributes: A multi-task network utilizing implicit and explicit relationships for facial attribute classification. In *AAAI*, 2017. 2, 6
- [16] B. Hassibi and D. G. Stork. Second order derivatives for network pruning: Optimal brain surgeon. In *NIPS*, 1993. 3
- [17] K. He, X. Zhang, S. Ren, and J. Sun. Deep residual learning for image recognition. In *CVPR*, 2016. 6
- [18] G. Hinton, O. Vinyals, and J. Dean. Distilling the knowledge in a neural network. *arXiv preprint arXiv:1503.02531*, 2015. 3
- [19] H. Hirschmuller. Stereo processing by semiglobal matching and mutual information. *TPAMI*, 30(2):328–341, 2008. 6
- [20] S. Huang, X. Li, Z. Cheng, A. Hauptmann, et al. Gnas: A greedy neural architecture search method for multi-attribute learning. 2018. 3, 5
- [21] Y. Ioannou, D. Robertson, J. Shotton, R. Cipolla, and A. Criminisi. Training cnns with low-rank filters for efficient image classification. *arXiv preprint arXiv:1511.06744*, 2015. 3
- [22] A. Jalali, S. Sanghavi, C. Ruan, and P. K. Ravikumar. A dirty model for multi-task learning. In *NIPS*, 2010. 2
- [23] S. Karayev, Y. Jia, J. Barron, M. Fritz, K. Saenko, and T. Darrell. A category-level 3-d object dataset: putting the kinect to work. In *CVPR Workshop*, 2011. 7
- [24] A. Kendall, Y. Gal, and R. Cipolla. Multi-task learning using uncertainty to weigh losses for scene geometry and semantics. In *CVPR*, 2018. 1, 2, 6
- [25] I. Kokkinos. Ubertnet: Training a universal convolutional neural network for low-, mid-, and high-level vision using diverse datasets and limited memory. In *CVPR*, 2017. 1
- [26] A. Kumar and H. Daume III. Learning task grouping and overlap in multi-task learning. 2012. 2
- [27] V. Lebedev and V. Lempitsky. Fast convnets using group-wise brain damage. In *CVPR*, 2016. 3
- [28] Y. LeCun, J. S. Denker, and S. A. Solla. Optimal brain damage. In *NIPS*, 1990. 3
- [29] J. Liang, E. Meyerson, and R. Miikkulainen. Evolutionary architecture search for deep multitask networks. In *GECCO*, 2018. 3
- [30] G. Lin, A. Milan, C. Shen, and I. Reid. Refinenet: Multi-path refinement networks for high-resolution semantic segmentation. In *CVPR*, 2017. 8
- [31] C. Liu, B. Zoph, M. Neumann, J. Shlens, W. Hua, L.-J. Li, L. Fei-Fei, A. Yuille, J. Huang, and K. Murphy. Progressive neural architecture search. In *ECCV*, 2018. 3
- [32] H. Liu, K. Simonyan, O. Vinyals, C. Fernando, and K. Kavukcuoglu. Hierarchical representations for efficient architecture search. *arXiv preprint arXiv:1711.00436*, 2017. 3
- [33] S. Liu, E. Johns, and A. J. Davison. End-to-end multi-task learning with attention. *arXiv preprint arXiv:1803.10704*, 2018. 1, 2, 6
- [34] S. Liu, S. J. Pan, and Q. Ho. Distributed multi-task relationship learning. In *ACM SIGKDD*, 2017. 2
- [35] Z. Liu, P. Luo, X. Wang, and X. Tang. Deep learning face attributes in the wild. In *ICCV*, 2015. 5
- [36] M. Long and J. Wang. Learning multiple tasks with deep relationship networks. *arXiv preprint arXiv:1506.02117*, 2015. 2
- [37] K. Lounici, M. Pontil, A. B. Tsybakov, and S. Van De Geer. Taking advantage of sparsity in multi-task learning. *arXiv preprint arXiv:0903.1468*, 2009. 2
- [38] Y. Lu, A. Kumar, S. Zhai, Y. Cheng, T. Javidi, and R. Feris. Fully-adaptive feature sharing in multi-task networks with applications in person attribute classification. In *CVPR*, 2017. 1, 2, 3, 4, 5, 6, 8
- [39] J.-H. Luo, J. Wu, and W. Lin. Thinet: A filter level pruning method for deep neural network compression. In *CVPR*, 2017. 3

- [40] I. Misra, A. Shrivastava, A. Gupta, and M. Hebert. Cross-stitch networks for multi-task learning. In *CVPR*, 2016. 1, 2, 5
- [41] D. Neven, B. De Brabandere, S. Georgoulis, M. Proesmans, and L. Van Gool. Fast scene understanding for autonomous driving. In *IEEE Symposium on Intelligent Vehicles 2017 Workshop*, 2017. 1, 2
- [42] S. J. Pan, Q. Yang, et al. A survey on transfer learning. *TKDE*, 22(10):1345–1359, 2010. 3
- [43] H. Pham, M. Y. Guan, B. Zoph, Q. V. Le, and J. Dean. Efficient neural architecture search via parameter sharing. In *ICML*, 2018. 3
- [44] E. Real, A. Aggarwal, Y. Huang, and Q. V. Le. Regularized evolution for image classifier architecture search. *arXiv preprint arXiv:1802.01548*, 2018. 3
- [45] A. Romero, N. Ballas, S. E. Kahou, A. Chassang, C. Gatta, and Y. Bengio. Fitnets: Hints for thin deep nets. *arXiv preprint arXiv:1412.6550*, 2014. 3
- [46] E. M. Rudd, M. Günther, and T. E. Boulton. Moon: A mixed objective optimization network for the recognition of facial attributes. In *ECCV*, 2016. 2, 6
- [47] S. Ruder. An overview of multi-task learning in deep neural networks. *arXiv preprint arXiv:1706.05098*, 2017. 2, 5
- [48] S. Ruder, J. Bingel, I. Augenstein, and A. Søgaard. Sluice networks: Learning what to share between loosely related tasks. *stat*, 1050:23, 2017. 1, 2
- [49] O. Sener and V. Koltun. Multi-task learning as multi-objective optimization. In *NIPS*, 2018. 1, 2, 5, 6, 7
- [50] N. Silberman, D. Hoiem, P. Kohli, and R. Fergus. Indoor segmentation and support inference from rgb-d images. In *ECCV*, 2012. 7
- [51] K. Simonyan and A. Zisserman. Very deep convolutional networks for large-scale image recognition. *arXiv preprint arXiv:1409.1556*, 2014. 5
- [52] S. Song, S. P. Lichtenberg, and J. Xiao. Sun rgb-d: A rgb-d scene understanding benchmark suite. In *CVPR*, 2015. 7
- [53] C. Tai, T. Xiao, Y. Zhang, X. Wang, et al. Convolutional neural networks with low-rank regularization. *arXiv preprint arXiv:1511.06067*, 2015. 3
- [54] J. Wang, Y. Cheng, and R. Schmidt Feris. Walk and learn: Facial attribute representation learning from egocentric video and contextual data. In *CVPR*, 2016. 6
- [55] J. Xiao, A. Owens, and A. Torralba. Sun3d: A database of big spaces reconstructed using sfm and object labels. In *CVPR*, 2013. 7
- [56] Y. Xue, X. Liao, L. Carin, and B. Krishnapuram. Multi-task learning for classification with dirichlet process priors. *JMLR*, 8(Jan):35–63, 2007. 2
- [57] M. Yuan and Y. Lin. Model selection and estimation in regression with grouped variables. *Journal of the Royal Statistical Society: Series B (Statistical Methodology)*, 68(1):49–67, 2006. 2
- [58] A. R. Zamir, A. Sax, W. Shen, L. J. Guibas, J. Malik, and S. Savarese. Taskonomy: Disentangling task transfer learning. In *CVPR*, 2018. 3, 4, 8
- [59] Z. Zhang, Z. Cui, C. Xu, Z. Jie, X. Li, and J. Yang. Joint task-recursive learning for semantic segmentation and depth estimation. In *ECCV*, 2018. 8
- [60] X. Zhao, H. Li, X. Shen, X. Liang, and Y. Wu. A modulation module for multi-task learning with applications in image retrieval. In *ECCV*, 2018. 1, 2, 6
- [61] J. Zhou, J. Chen, and J. Ye. Malsar: Multi-task learning via structural regularization. *Arizona State University*, 21, 2011. 2
- [62] B. Zoph and Q. V. Le. Neural architecture search with reinforcement learning. *arXiv preprint arXiv:1611.01578*, 2016. 3